

onances appear throughout the temperature range investigated.

The reaction involving benzenethiol proceeds in much the same manner except that an additional species (**11**) appears at $-80\text{ }^{\circ}\text{C}$, together with **9** and **10**, which appear exactly analogous to **7** and **8**, respectively. Compound **11** displays a hydride resonance, a broad singlet at $\delta -10.65$, in the ^1H NMR spectrum, and selective ^{31}P decoupling shows that it is bound only to Re, since no effect is observed on irradiating the Rh-bound phosphorus nuclei, whereas collapse to a narrower signal is observed when the Re-bound phosphorus nuclei are decoupled. The $^{13}\text{C}\{^1\text{H}\}$ NMR spectrum also shows that this intermediate is a tetracarbonyl. We therefore propose the structure shown in Scheme II for **11**. Although we cannot unambiguously establish whether the thiolato group and the hydride ligand are on opposite faces of the dimer, as shown, this appears reasonable on the basis of the structure determination of **5**.

It is apparent that the initial stages in the reactions of **1** with H_2S and thiols are analogous. We first observe the simple HSR ($\text{R} = \text{H, Et, Ph}$) adducts, in which these groups presumably coordinate at the unsaturated Rh center, followed by oxidative addition to yield a bridging hydride species. Not unexpectedly, the pathways involving H_2S and the thiols begin to diverge after this, since for H_2S , oxidative addition of the second H–S linkage can occur, whereas the analogous process is much less facile for the R–S linkage of the thiolato group. An intermediate such as **11**, which was only observed for HSPH, may also be important in the second oxidative addition of H_2S , since, as formulated, this yields a coordinatively unsaturated Rh(I) center that can then oxidatively add to the coordinated S–H moiety, giving a dihydride species which then reductively eliminates H_2 very readily. In the case of the thiols, for which the second oxidative addition reaction does not occur, another pathway, in which the terminal thiolato group on Rh forms a dative bond to Re with expulsion of CO, becomes favorable.

Throughout these studies we find no evidence that the Re atom is directly involved in the oxidative addition reactions. However

it is clear that this atom plays a significant role. It appears that Re can serve to generate coordinative unsaturation at Rh after the first oxidative addition step, both by cleavage of the Re–Rh dative bond and possibly by accepting a hydrido ligand, as shown in the HSPH reaction (species **11**). By contrast, the mononuclear complexes $[\text{RhCl}(\text{PPh}_3)_3]$ and $[\text{IrCl}(\text{CO})(\text{PPh}_3)_2]$ were also found to undergo the first oxidative addition step with H_2S ,⁴ but in neither case did oxidative addition of the second S–H bond occur, presumably since the products of the first oxidative additions were in the +3 oxidation states and were much less prone to further oxidative addition. Subsequent reaction of compound **4**, via transfer of the hydride ligand to Re yielding a species analogous to **11**, is akin to reductively eliminating the “ $\text{HRe}(\text{CO})_3\text{P}_2$ ” moiety to regenerate a Rh(I) center, which is again capable of oxidatively adding to the second S–H bond. The structure determination of **5** also lends support to the idea that facile electron and ligand reorganization over the central core can occur. Although the thiolato group in intermediate **11** is apparently bound to Rh with the hydride on Re, the reverse appears more appropriate in **5**, with the hydride ligand more closely associated with Rh and the thiolate more tightly bound to Re. Such reorganization is clearly important in promoting reactivity in these mixed-metal systems.

Currently we are attempting to obtain additional information on the intermediates in such reactions with aims of learning more about the involvement of the Re center in this chemistry.

Acknowledgment. We thank the Natural Sciences and Engineering Research Council of Canada (NSERC) and the University of Alberta for financial support and NSERC for partial support for the purchase of the diffractometer and for funding of the PE883 IR spectrometer.

Supplementary Material Available: Tables giving anisotropic thermal parameters, additional bond lengths and angles, hydrogen atom parameters, a summary of crystallographic data, and positional parameters for all atoms (9 pages); listings of the observed and calculated structure factors (26 pages). Ordering information is given on any current masthead page.

Contribution from the Department of Chemistry,
University of Missouri—Columbia, Columbia, Missouri 65211

Syntheses of Monomeric (η^5 -Pentamethylcyclopentadienyl)platinum(IV) Methyl and Bromo Complexes and of [Hydrotris(3,5-dimethyl-1-pyrazolyl)borato]trimethylplatinum

Steven Roth, Visalakshi Ramamoorthy,[†] and Paul R. Sharp*

Received January 24, 1990

The reaction of $\text{Cp}^*\text{MgCl}\cdot\text{THF}$ ($\text{Cp}^* = \text{C}_5\text{Me}_5$) with 1 equiv of PtMe_3I and PtMe_2Br_2 produces Cp^*PtMe_3 (**1**) and $\text{Cp}^*\text{PtMe}_2\text{Br}$ (**2**), respectively. Reaction of **2** with Br_2 produces $\text{Cp}^*\text{PtMeBr}_2$ (**3**) in good yield. The structures of **2** and **3** have been determined by X-ray crystallography. Complex **2** crystallizes in the monoclinic space group, $P2_1/m$, with $a = 7.017$ (4) Å, $b = 11.573$ (4) Å, $c = 8.496$ (3) Å, $\beta = 98.59$ (3) $^{\circ}$, $Z = 2$, $V = 682.1$ Å³, $R = 0.067$, and $R_w = 0.081$. Complex **3** also crystallizes in the monoclinic space group, $P2_1/m$, with $a = 7.147$ (2) Å, $b = 12.171$ (4) Å, $c = 8.617$ (2) Å, $\beta = 113.77$ (2) $^{\circ}$, $Z = 2$, $V = 685.9$ Å³, $R = 0.036$, and $R_w = 0.053$. The molecules reside on mirror planes and are monomeric pseudotetrahedral Pt(IV) complexes with “piano stool” type geometries and η^5 -Cp* groups. Both molecules have Br atoms on the mirror. This leads to a disorder of the Me and the second Br positions in complex **3**. The average Pt–C(Cp*) bond length is 2.25 (7) Å in **2** and 2.22 (4) Å in **3**. The Pt–C(Me) and Pt–Br bond lengths in **2** are 2.07 (2) and 2.498 (2) Å, respectively. The ordered Pt–Br bond length in **3** is 2.496 (2) Å. Treatment of **1** with halogens results in the cleavage of the Pt–Cp* bond. The reaction of PtMe_3I with KTP^* ($\text{TP}^* = [\text{HB}(3,5\text{-dimethylpyrazolyl})_3]^-$) in thf gives TP^*PtMe_3 (**4**) in almost quantitative yield. The reaction of **4** with Br_2 brominates the 4-position of the pyrazolyl ring only.

Introduction

While the organometallic chemistry of the group VIII metals Rh and Ir with the Cp* ($\text{Cp}^* = \text{C}_5\text{Me}_5$) ligand has rapidly developed over the past 10–15 years, that of analogous Pt systems has progressed little.^{1–4} A major obstacle to development of the Pt systems is the absence of the Pt analogue of $[\text{Cp}^*\text{MCl}_2]_2$ (M

= Rh, Ir), the major starting material for the Rh and Ir systems. Although a Cp* bromo complex of Pt(IV) has been reported, it is obtained in poor yield and is poorly characterized.⁵ In this

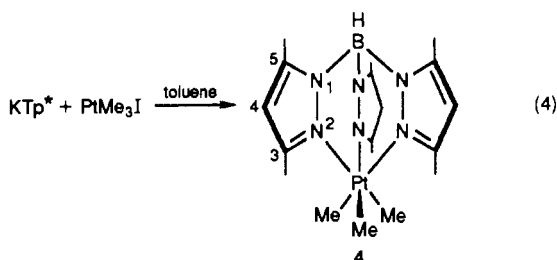
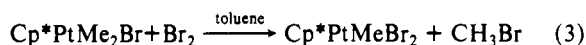
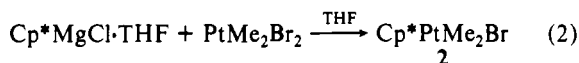
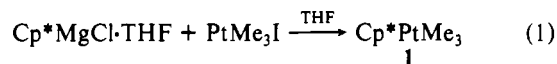
- (1) Maitlis, P. M. *Acc. Chem. Res.* **1978**, *11*, 307.
- (2) Maitlis, P. M. *Chem. Soc. Rev.* **1981**, *10*, 1.
- (3) Isobe, K.; Bailey, P. M.; Maitlis, P. M. *J. Chem. Soc., Dalton Trans.* **1981**, 2003.
- (4) McGhee, W. D.; Foo, T.; Hollander, F. J.; Bergman, R. G. *J. Am. Chem. Soc.* **1988**, *110*, 8543.
- (5) Taylor, S.; Maitlis, P. M. *J. Organomet. Chem.* **1977**, *139*, 121.

[†]Permanent address: Chemistry Division, BARC, Trombay, Bombay 400085, India.

paper we report the preparation and characterization of Cp^*PtMe_3 (**1**),⁶ $\text{Cp}^*\text{PtMe}_2\text{Br}$ (**2**), $\text{Cp}^*\text{PtMeBr}_2$ (**3**), and Tp^*PtMe_3 (**4**), which should aid in the development of PtCp^* chemistry. Since Tp^* ($\text{Tp}^* = [\text{HB}(3,5\text{-dimethylpyrazolyl})_3]^-$) counterparts of Cp^* compounds are known,⁷ we have also synthesized Tp^*PtMe_3 and briefly explored its derivatization.

Results

Compounds **1**–**4** are air stable and can be prepared according to eqs 1–4. The Cp^* Grignard reactions (eqs 1 and 2) darken

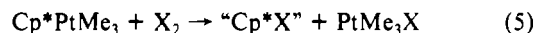


considerably as they proceed, and Cp^*H is detected on work-up. This, and the relatively low yields, suggest some reduction of the Pt(IV) . Similar observations have been reported for Cp^* Grignard reactions with Pt(II) complexes.⁸ Unlike the Cp^*Pt compounds, the Tp^*Pt compound, **4**, can be isolated in greater than 90% yield.

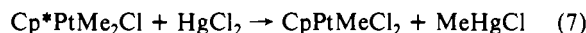
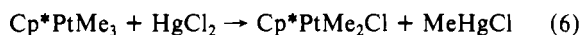
Compound **1** is colorless and extremely volatile and readily sublimates at room temperature and 10^{-2} mmHg. It is highly soluble in aromatic, aliphatic, and chlorinated solvents. These properties complicate its isolation and probably contribute to its low yield. In contrast, compound **2** is relatively nonvolatile and is readily recovered from diethyl ether or hexane as yellow crystals.

Compound **3** has low solubility in hydrocarbons and precipitates as a red solid from yellow toluene solutions of **2** that are exposed to bromine (eq 3). It is moderately soluble in methylene chloride and less soluble in chloroform.

Compound **1** also reacts with halogens (Br_2 and Cl_2). However, in contrast to the case of **2**, the Pt-Cp^* bond is attacked and PtMe_3X ($\text{X} = \text{Br}, \text{Cl}$) is observed (eq 5; $\text{X} = \text{Br}, \text{Cl}$). When excess



HgCl_2 is added to a CDCl_3 solution of **1**, a slow reaction occurs according to eqs 6 and 7.



The ^1H and ^{13}C NMR parameters of the Cp^* groups in the above complexes are comparable to $(\text{MeCp})\text{PtMe}_3$ ⁹ and are within the range reported for $\text{Cp}^*\text{Pt}^{\text{II}}$ complexes such as $\text{Cp}^*_2\text{Pt}_2(\text{CO})_2$, $\text{Cp}^*\text{Pt}(\text{CODCp}^*)$, and $\text{Cp}^*\text{Pt}(\text{CO})\text{Cl}$.⁸ Consistent with the greater basicity of the Cp^* ligand, the 0.35 ppm chemical shift (CDCl_3) of the Pt-Me groups in **1** appears to be shielded as compared to those of CpPtMe_3 (0.92 ppm)¹⁰ and $(\text{MeCp})\text{PtMe}_3$ (0.83 ppm).⁹ The Pt-H (Pt-Me) coupling constants of **1**–**4** are

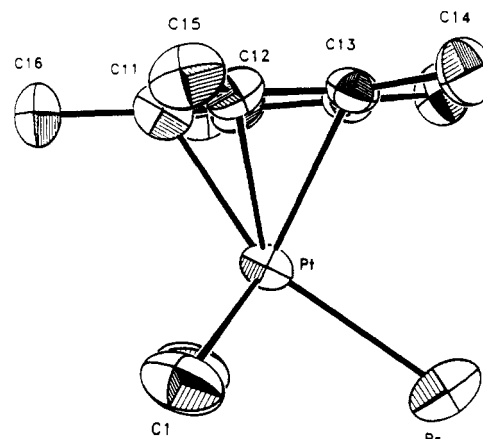


Figure 1. Perspective diagram (ORTEP) of $\text{Cp}^*\text{PtMe}_2\text{Br}$ (**2**) viewed normal to the mirror with 50% probability thermal ellipsoids.

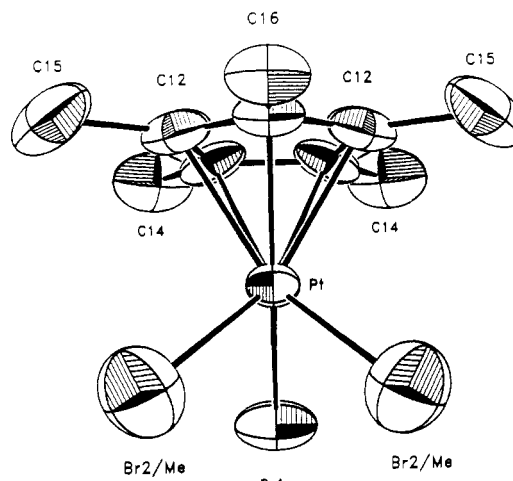


Figure 2. Perspective diagram (ORTEP) of $\text{Cp}^*\text{PtMeBr}_2$ (**3**) with 50% probability thermal ellipsoids.

also within the range of those reported for tetrameric Pt(IV) alkyls¹¹ and for the monomeric $\eta^5\text{-Cp}$ and MeCp class of Pt(IV) organometallics.^{9,12,13}

The ^1H NMR spectrum of **4** is devoid of an H-B peak, presumably due to quadrupolar broadening by ^{11}B , but does consist of singlets for each other type of proton: δ (ppm) = 5.73 (4-H-pz), 2.34, 2.38 (3,5-Me₂-pz), and 1.32 (Pt-Me , $J_{\text{Pt-H}} = 70$ Hz). Upon addition of Br_2 to a toluene solution of **4**, the peak due to the 4-H of the pyrazolyl ring disappears and a downfield shift (δ (ppm) = 2.61, 2.41, and 1.50 ($J_{\text{Pt-H}} = 86$ Hz)) and larger $J_{\text{Pt-H}}$ values are observed for the other signals. Since no CH_3Br nor any intensity changes in the Pt-Me peak were observed, only the 4-H pyrazolyl ring position was brominated. Trofimenko et al. have brominated the 4-H position of 3-isopropylpyrazole prior to the synthesis of the polypyrazolylborate species.¹⁴

Description of the Structures. Perspective drawings of $\text{Cp}^*\text{PtMe}_2\text{Br}$ (**2**) and $\text{Cp}^*\text{PtMeBr}_2$ (**3**) are shown in Figures 1 and 2, respectively. In both structures the Cp^* ligand is coordinated to the Pt(IV) in an η^5 fashion to give molecules of the CpML_3 "piano stool" type. The molecules lie on mirror planes that pass through Br , Pt , $\text{C}(11)$, $\text{C}(16)$, and the bisector of the $\text{C}(13)\text{-C}(13)$ bond of each structure. The $\text{Pt-C}(\text{Me})$ distance, 2.07 (2) Å, in **2** is similar to those found in $[(\text{Me}_3\text{Pt}(\text{OH}))_4]^{15}$

(6) Yang et al. have recently reported the synthesis of Cp^*PtMe_3 , using LiCp^* in place of the Grignard reagent in eq 1: Yang, D. S.; Bancroft, G. M.; Puddephatt, R. J.; Bursten, B. E.; McKee, S. D. *Inorg. Chem.* **1989**, *28*, 872.
 (7) Trofimenko, S. *Prog. Inorg. Chem.* **1986**, *34*, 115.
 (8) Boag, N. M. *Organometallics* **1988**, *7*, 1446.
 (9) Ziling, X.; Strouse, J.; Shuh, D. K.; Knobler, C. B.; Kaesz, H. D.; Hicks, R. F.; Williams, R. S. *J. Am. Chem. Soc.* **1989**, *111*, 8779.
 (10) Robinson, S. D.; Shaw, B. L. *J. Chem. Soc.* **1965**, 1529.

(11) Jain, V. K.; Rao, G. S.; Jain, L. *Adv. Organomet. Chem.* **1987**, *27*, 113.
 (12) Shaver, A. *Can. J. Chem.* **1978**, *56*, 2281.
 (13) Hamer, G.; Shaver, A. *Can. J. Chem.* **1980**, *58*, 2011.
 (14) Trofimenko, S.; Calabrese, J. C.; Domaille, P. J.; Thompson, J. S. *Inorg. Chem.* **1989**, *28*, 1091.
 (15) (a) Spiro, T. G.; Templeton, D. H.; Zalkin, A. *Inorg. Chem.* **1965**, *7*, 2165. (b) Preston, H. S.; Mills, J. C.; Kennard, C. H. L. *J. Organomet. Chem.* **1968**, *14*, 447.

and $[(\text{Me}_3\text{PtBr})_4] \cdot 0.5\text{tol}$ (tol = toluene).¹⁶ The Pt–Br distances, 2.498 (2) Å (2) and 2.496 (2) Å (3, Pt–Br(1)), are similar to the terminal Pt–Br distances in $[\text{Pt}(\text{en})\text{Br}_3]$ (a complex between $[\text{Pt}(\text{en})\text{Br}_2]$ and $[\text{Pt}(\text{en})\text{Br}_4]$), 2.51 (4) Å (Pt(II)) and 2.48 (1) Å (Pt(IV)),¹⁷ *trans*- $[(\text{PEt}_3)_2\text{PtBr}_2]$, 2.428 (2) Å,¹⁸ $(\text{PEt}_3)_2\text{PtHBr}$, 2.56 (4) Å,¹⁹ and *trans*- $(\eta^1\text{-C}_3\text{H}_5)\text{PtBr}(\text{PEt}_3)_2$, 2.543 (1) Å,²⁰ but shorter than the 2.677 (3) Å bridging Pt–Br distance in $[(\text{Me}_3\text{PtBr})_4] \cdot 0.5\text{tol}$.¹⁶

The average Pt–C(Cp*) distances, 2.25 (7) Å (2), and 2.22 (4) Å (3), are similar to those found in CpPtMe_3 ,²¹ MeCpPtMe_3 ,⁹ and $\text{Cp}^*\text{Pt}_2(\text{CO})_2$ ⁸ but range from 2.14 (2) to 2.33 (1) Å in complex 2 and from 2.17 (1) to 2.25 (1) Å in 3 (Table III). This wide range of Pt–C(Cp*) distances may be caused by steric interactions or the differing trans influence of the Me and Br ligands. A trans influence in Cp* complexes has previously been observed to give large ranges in the M–C(Cp*) distances. The resulting distortion is described as a ring slippage, that is, a displacement of the metal from the ring center.²² Alternatively, it can be described as a tilt of the ring about the ring centroid. We prefer this alternative description for 2. The ring is essentially planar (deviations range from –0.03 (2) to 0.03 (1) Å, Table SV (supplementary material)) and tilts “up” from the mirror plane Br atom as shown by the 84° angle formed by the Pt–Cp*(centroid) vector and the plane of the C₅ ring in the direction of C(11). This should result from the weaker (as compared to Me) trans influence of the Br ligand on C(11) which is “trans” to the Br ligand. Indeed, C(11) is the ring carbon with the shortest Pt–C distance. This shortened distance occurs despite an unfavorable steric interaction, as indicated by the very small 3.44 Å intramolecular contact between the methyl group on C(11) (C(15)) and C(1). As a result, C(15) is bent 0.12 (1) Å out of the C₅ plane away from the Pt–L₃ tripod (cf. 0.05 (1) Å for C(14) and 0.06 (1) Å for C(16), Table SV). The ring tilt could also result from the large size of the Br atom “pushing” the ring up (Br...C(13) = 3.62 Å and Br...C(14) = 3.85 Å), but the counterring C(15)–C(1) contact seems to be more strained than would be expected and we feel the difference in trans influence is the more likely explanation. A similar situation may occur in 3, but unfortunately, the disorder in 3 precludes a detailed analysis.

Concluding Remarks

To date, there are only a handful of monomeric Pt(IV) organometallic compounds reported. Those which contain an η⁵-Cp group have in the three remaining coordination sites three alkyl or one acyl and two alkyl ligands. These complexes might be useful precursors to other CpPt complexes if the alkyl and/or acyl ligands could be replaced with halogens. However, the Pt–Cp bond in these complexes is more susceptible to electrophilic metal–carbon bond cleavage than the Pt–alkyl and/or –acyl bonds. For example, CpPtMe_3 , the Cp analogue of 1, reacts with X₂ or HgX₂ (X = halogen) to give Cp*X and PtMe₃X.¹² Similar results are obtained with Cp*PtMe₃ (1) although the Pt–Cp* bond is less susceptible to cleavage with HgX₂.

However, a striking difference is observed with Cp*PtMe₂Br (2). The bromine ligand has greatly reduced the susceptibility of the Cp*–Pt bond to electrophilic cleavage. In fact, solutions of 2 exposed to excess Br₂ for several hours give only 3. Prolonged exposure of 3 to excess Br₂ vapor does give a small amount of a highly insoluble brick red solid along with unreacted 3. A highly insoluble compound, formulated as $[\text{Cp}^*\text{PtBr}_3\text{PtCp}^*]\text{Br}_3$, has been prepared in low yield by Taylor and Maitlis.⁵ Since we have been

unable to dissolve this material in conventional NMR solvents, it may be the same material reported earlier by Taylor and Maitlis. Finally, we note that thus far our efforts to prepare amido compounds from 2 and 3 via metathesis reactions with, for example, LiNHR (R = *tert*-butyl or phenyl) gave back low yields of starting materials and no tractable products.

In contrast to the case of the Cp and Cp* complexes, stoichiometric and excess Br₂ at 22 °C only brominates the 4-position of the pyrazolyl ring of Tp*PtMe₃. The Pt–Me or Tp*–N–Pt bonds are not cleaved. The Pt–Me bonds may be cleaved under more severe conditions, but it is questionable whether the Tp* ligand could survive.

Experimental Section

Materials and Methods. Preparations of 1–4 were performed under a dry nitrogen atmosphere by using normal Schlenk techniques and a Vacuum Atmospheres glovebox equipped with an HE-493 Dri-train. Solvents were dried over sodium benzophenone ketyl and were distilled prior to use. Infrared spectra (4000–600 cm^{–1}) were recorded on a Nicolet 20-DXB spectrometer. Samples were prepared as thin-film solids on NaCl plates. ¹H (300 MHz), ¹³C (75 or 22.45 MHz), and ¹¹B (96.3 MHz) NMR spectra were recorded at ambient temperature on a Nicolet NM-300 or JEOL FX-90 spectrometer operating in the Fourier transform mode. Chemical shifts are referenced to internal deuterated solvents (¹H and ¹³C), recalculated to TMS = 0.0 ppm, and external BF₃·O(C₂H₅)₂ (=0.0 ppm (¹¹B)). Elemental analyses were performed by Oneida Research Services, Whitesboro, NY. Trimethylplatinum iodide,²³ dimethylplatinum dibromide,²⁴ pentamethylcyclopentadiene, Cp*H,²⁵ and its Grignard reagent Cp*MgCl·THF,²⁶ and KTp*²⁷ were prepared according to literature procedures.

Syntheses. Cp*PtMe₃ (1). To a slurry of 0.50 g (1.36 mmol) of PtMe₃I in THF (20 mL) was added 0.36 g (1.36 mmol) of Cp*MgCl·THF in about 10 mL of THF. After being stirred for a few minutes at room temperature, the solution had changed from a light yellow to black color (probably reflecting partial reduction of Pt(IV)). The solution was stirred for 24 h, and then the solvent was allowed to evaporate in air, leaving a dry black residue. The product was extracted from the dark residue with 3 × 10 mL of hexane, and the extract was filtered through a medium-porosity glass frit, giving a clear yellow solution. The solution was concentrated to near dryness by slow evaporation in air. The yellow supernatant, containing some free Cp*H, was decanted, leaving colorless crystalline 1. Yield: 25–40%.

¹H NMR (CDCl₃), δ: 1.73 (15 H, m, ³J_{Pt-H} = 8 Hz), Cp*; 0.35 (9 H, m, ²J_{Pt-H} = 79 Hz). ¹³C{¹H} NMR (22.49 MHz, CDCl₃), δ: 101.8, C₅ (Cp*); 7.7, Me (Cp*); –11.0 (*J*_{Pt-C} = 710 Hz), Pt–Me. IR: 2950 (sh), 2922 (m), 2893 (sh), 2876 (s), 2800 (s), 1450 (m), 1421 (m), 1377 (s), 1258 (s), 1238 (s), 1220 (m), 1200 (s), 1026 (w), 909 (s), 852 (w), 796 (w), 733 (s) cm^{–1}.

Reaction of 1 with HgCl₂. To an NMR tube containing 20 mg (0.053 mmol) of Cp*PtMe₃ in CDCl₃ was added 54 mg (0.20 mmol) of HgCl₂. As monitored by ¹H NMR spectroscopy, no changes occurred within the first several hours. After 3 days, the spectrum showed peaks due to 1 and new Pt–Cp* (δ = 1.78, *J*_{Pt-H} = 16 Hz, 15 H) and Pt–Me (δ = 1.15, *J*_{Pt-H} = 78 Hz, 6 H) peaks, along with those due to MeHgCl (1.13 ppm, *J*_{Hg-H} = 201 Hz). After several more days, the peaks due to 1 were no longer present, the MeHgCl peaks increased in intensity, and new Pt–Cp* (δ = 1.85, *J*_{Pt-H} = 17 Hz, 15 H) and Pt–Me peaks (δ = 1.87, *J*_{Pt-H} = 78 Hz, 3 H) were present. By integration and analogy to 2 and 3 below, these latter two compounds are assigned to Cp*PtMe₂Cl and Cp*PtMeCl₂, respectively. After ca. 4 weeks, only the MeHgCl peaks and the upfield set of Pt–Cp* and Pt–Me peaks assigned to Cp*PtMeCl₂ were present.

Reaction of 1 with X₂ (X = Cl, Br). To an NMR tube containing ca. 20 mg of 1 in CDCl₃ was injected ca. 3 equiv of Cl₂. The ¹H NMR spectrum, within several minutes after injection, contained only Pt–Me peaks due to PtMe₃Cl and a complex Cp* region devoid of ¹⁹⁵Pt coupling. In an analogous reaction with Br₂, only Pt–Me peaks due to PtMe₃Br were observed.

Cp*PtMe₂Br (2). To a slurry of 0.10 g (2.6 mmol) of PtMe₂Br₂ in THF (5 mL) was added 0.70 g (2.6 mmol) of Cp*MgCl·THF in about 4 mL of THF. The solution turned black after a few minutes and was

(16) Massa, W.; Baum, G.; Seo, B.-S.; Lorberth, J. *J. Organomet. Chem.* **1988**, *352*, 415.

(17) Ryan, T. D.; Rundle, R. E. *J. Am. Chem. Soc.* **1961**, *83*, 2814.

(18) Messmer, G. G.; Amma, E. L. *Inorg. Chem.* **1966**, *5*, 1775.

(19) Owston, P. G.; Partridge, J. M.; Rowe, J. M. *Acta Crystallogr.* **1960**, *13*, 246.

(20) Huffman, J. C.; Laurent, M. P.; Kochi, J. K. *Inorg. Chem.* **1977**, *16*, 2639.

(21) Adamson, G. W.; Bart, J. C. J.; Daly, J. J. *J. Chem. Soc.* **1971**, 2616.

(22) Herrmann, W. A.; Herdtweck, E.; Flöel, M.; Kulpe, J.; Küsthardt, U.; Okuda, J. *Polyhedron* **1987**, *6*, 1165.

(23) Baldwin, J. C.; Kaska, W. C. *Inorg. Chem.* **1975**, *14*, 2020.

(24) Hall, J. R.; Hirons, D. A.; Swile, G. A. *Inorg. Synth.* **1980**, *20*, 185.

(25) (a) Kohl, F. X.; Jutzi, P. *J. Organomet. Chem.* **1983**, *243*, 119. (b) Fietler, D.; Whitesides, G. M. *Inorg. Chem.* **1976**, *15*, 466.

(26) Fagan, P. J.; Manriquez, J. M.; Maata, E. A.; Seyam, A. F.; Marks, T. J. *J. Am. Chem. Soc.* **1981**, *103*, 6650.

(27) Trofimenko, S. *J. Am. Chem. Soc.* **1967**, *89*, 6288.

Table I. Crystallographic Data for Cp*PtMe₂Br (2) and Cp*PtMeBr₂ (3)

	2	3
formula	C ₁₂ H ₂₁ PtBr	C ₁₁ H ₁₈ PtBr ₂
space group	P2 ₁ /m	P2 ₁ /m
fw	440.09	505.16
a, Å	7.017 (4)	7.147 (2)
b, Å	11.573 (4)	12.171 (4)
c, Å	8.496 (3)	8.617 (2)
β	98.59 (3)	113.77 (2)
V, Å ³	682.1	685.9
Z	2	2
T, °C	21	21
λ, Å	0.71069	0.17069
ρ _{calcd} , g cm ⁻³	2.14	2.45
μ, cm ⁻¹	132.28	189.28
transm coeff	0.562–0.998	0.685–1.000
R(F _o)	0.067	0.036
R _w (F _o)	0.081	0.053

Table II. Positional Parameters and Isotropic Equivalent Thermal Parameters for Cp*PtMe₂Br (2)

atom	x	y	z	B, Å ²
Pt	0.01381 (7)	0.250	0.22755 (7)	2.49 (1)
Br	-0.2567 (3)	0.250	0.0002 (3)	4.57 (4)
C(1)	-0.129 (2)	0.132 (1)	0.350 (2)	4.8 (3)
C(11)	0.305 (2)	0.250	0.346 (2)	3.2 (3)
C(12)	0.293 (1)	0.149 (1)	0.245 (1)	2.8 (2)
C(13)	0.254 (1)	0.186 (1)	0.088 (1)	2.9 (2)
C(14)	0.229 (2)	0.115 (1)	-0.059 (2)	4.2 (3)
C(15)	0.317 (2)	0.027 (1)	0.300 (2)	3.9 (3)
C(16)	0.356 (3)	0.250	0.524 (2)	4.7 (5)

stirred overnight. The solvent was removed in vacuo, and the residue was extracted with 3 × 25 mL of toluene. The resulting solution was filtered through a column of diatomaceous earth. The yellow filtrate was concentrated to dryness in vacuo. Crystals, suitable for X-ray analysis, were obtained by dissolving the orange-yellow solid in a minimum volume of ether followed by cooling at -20 °C overnight. The supernatant was decanted, and the crystals were dried in vacuo. A second crop was obtained in a similar manner from the supernatant. Total yield: 0.71 g (62%).

¹H NMR (CDCl₃, 21 °C), δ: 1.84 (15 H, m, ³J_{Pt-H} = 16 Hz), Cp*; 1.23 (6 H, m, ²J_{Pt-H} = 78 Hz). ¹³C{¹H} NMR (22.49 MHz, CDCl₃), δ: 106.3 (J_{Pt-C} = 16 Hz), C₅ (Cp*); 7.93, Me (Cp*); -2.9 (J_{Pt-C} = 691 Hz), Pt-Me. IR: 2975 (m), 2960 (m), 2893 (s), 1524 (s), 1415–1444 (br, w), 1375 (s), 1315 (m), 1260 (w), 1220 (s), 1150 (m), 1020 (s) cm⁻¹. Anal. Calcd (found) for C₁₂H₂₁PtBr: C, 32.73 (32.73); H, 4.81 (4.73).

Cp*PtMeBr₂ (3). Bromine vapor was passed over a yellow toluene solution (20 mL) of Cp*PtMe₂Br (0.420 g, 0.95 mmol). The solution immediately turned red, and after a few minutes a deep red solid precipitated. The red precipitate was separated out by filtration, washed with ca. 5 mL of hexane, and dried in vacuo. Crystals suitable for X-ray analysis were obtained by slow diffusion of ether into a CH₂Cl₂ solution of 3 kept at -20 °C over several days. The supernatant was decanted, and the crystals were dried in vacuo. Slow evaporation of the supernatant gave a second crop. Total yield: 0.37 g (77%).

¹H NMR (CDCl₃, 21 °C), δ: 1.92 (15 H, m, ³J_{Pt-H} = 17 Hz), Cp*; 1.96 (3 H, m, ²J_{Pt-H} = 86 Hz). ¹³C{¹H} NMR (75 MHz, CDCl₃), δ: 110.7 (J_{Pt-C} = 41 Hz), C₅ (Cp*); 8.9, Me (Cp*); 6.0 (J_{Pt-C} = 680 Hz), Pt-Me. IR: 2959 (m), 2910 (s), 2853 (m), 1525 (w), 1471 (m), 1437 (m), 1412 (w), 1367 (m), 1344 (m), 1217 (m), 1190 (m), 1153 (m), 1000 (m) cm⁻¹. Anal. Calcd (found) for C₁₁H₁₈PtBr₂: C, 26.15 (26.51); H, 3.59 (3.58).

Tp*PtMe₃ (4). To a slurry of 0.30 g (0.82 mmol) of PtMe₃I in THF (5 mL) was added 0.28 g (0.83 mmol) of KTp* in about 5 mL of THF. The solution was stirred for 24 h, and then the solvent was removed in vacuo to give a light-colored residue. The product was separated from KI by extraction with 3 × 2 mL of toluene, and the extract was filtered through a medium-porosity glass frit containing Celite filter aid, giving a clear solution. The solvent was removed, leaving a colorless crystalline solid. Yield: 0.41 g (93%).

¹H NMR (CDCl₃), δ: 5.73 (3 H, s), 4-Hpz: 2.34 (9 H, s), 2.28 (9 H, s), 3,5-Me₂pz: 1.32 (9 H, m, ²J_{Pt-H} = 70 Hz), Pt-Me. ¹³C{¹H} NMR (22.49 MHz, CDCl₃), δ: 149.2, 143.0, 107.6, C₃ (pz); 13.1, 12.8, 3,5-Me₂pz; -10.5 (J_{Pt-C} = 686 Hz), Pt-Me. ¹¹B NMR (CDCl₃), δ: -9.89 (d, J_{B-H} = 89 Hz). IR: ν_{B-H} = 2520 cm⁻¹. Anal. Calcd (found) for C₁₈H₃₁N₆PtB: C, 40.23 (40.46); H, 5.81 (5.89); N, 15.64 (15.41).

Table III. Positional Parameters and Isotropic Equivalent Thermal Parameters for Cp*PtMeBr₂ (3)

atom	x	y	z	B, Å ²
Pt	0.13716 (6)	0.250	0.22662 (6)	2.872 (9)
Br(1)	-0.2350 (2)	0.250	0.0372 (2)	5.95 (5)
Br(2) ^a	0.0824 (3)	0.3794 (2)	0.4238 (3)	5.06 (5)
C(11)	0.464 (2)	0.250	0.294 (2)	4.5 (4)
C(12)	0.387 (11)	0.346 (1)	0.192 (1)	4.8 (2)
C(13)	0.253 (1)	0.310 (1)	0.035 (1)	4.1 (2)
C(14)	0.128 (2)	0.377 (1)	-0.127 (1)	6.8 (3)
C(15)	0.443 (2)	0.463 (2)	0.239 (3)	12.1 (5)
C(16)	0.616 (2)	0.250	0.478 (3)	8.1 (8)
C(1) ^a	0.091	0.360	0.395	4.0

^aBr(2) and C(1) are the disordered bromine and methyl carbon. Both were assigned occupancy 0.5, with Br(2) allowed to refine and C(1) placed and fixed at a reasonable Pt-C distance along the Pt-Br(2) vector.

Table IV. Bond Distances (Å) for Cp*PMe₂Br (2) and Cp*PtMeBr₂ (3)

	2	3
Pt-Br(1)	2.498 (2)	2.496 (2)
Pt-C(1)	2.07 (2)	2.1 ^a
Pt-Br(2)		2.462 (2)
Pt-C(11)	2.14 (2)	2.17 (1)
Pt-C(12)	2.27 (1)	2.252 (9)
Pt-C(13)	2.33 (1)	2.247 (8)
C(11)-C(12)	1.45 (2)	1.43 (2)
C(11)-C(16)	1.50 (2)	1.52 (2)
C(12)-C(13)	1.40 (1)	1.38 (1)
C(11)-C(15)	1.49 (2)	1.49 (2)
C(13)-C(13)'	1.48 (2)	1.45 (2)
C(13)-C(14)	1.50 (2)	1.55 (2)
Pt-Cp ^b	1.909	1.852

^aBr(2) and C(1) are the disordered Br and methyl carbon atoms, and C(1) was included in the model at a calculated and fixed position along the Pt-Br(2) vector. The Br(2)-C(1) distance is 0.36 Å. Atoms marked with a prime are related by the mirror. ^bCp represents the centroid of the C₅ ring.

Table V. Bond Angles (deg) for Cp*PtMe₂Br (2) and Cp*PtMeBr₂ (3)

	2	3
Br(1)-Pt-C(1)	91.1 (4)	
Br(1)-Pt-Br(2) ^a		91.55 (6)
Br(1)-Pt-C(11)	157.8 (5)	157.4 (4)
Br(1)-Pt-C(12)	126.8 (3)	127.3 (3)
Br(1)-Pt-C(13)	97.4 (3)	97.6 (2)
Br(2)-Pt-C(1)'		79.7 ^a
Br(2)-Pt-C(11)		105.6 (3)
Br(2)-Pt-C(12)		96.5 (3)
Br(2)-Pt-C(13)		120.5 (3)
C(1)-Pt-C(11)	105.4 (5)	
C(1)Pt-C(12)	96.0 (5)	
C(1)-Pt-C(13)	119.5 (5)	
C(11)-Pt-C(12)	38.2 (4)	37.8 (3)
C(11)-Pt-C(13)	61.7 (6)	61.2 (4)
C(12)-Pt-C(13)	35.4 (4)	35.7 (4)
C(13)-Pt-C(13)'	36.9 (4)	37.7 (4)
Pt-C(11)-C(12)	75.6 (8)	74.3 (6)
Pt-C(11)-C(16)	123 (1)	121 (1)
C(12)-C(11)-C(16)	125.6 (7)	125.1 (6)
C(12)-C(11)-C(12)'	108 (1)	110 (1)
Pt-C(12)-C(11)	66.2 (7)	67.9 (6)
Pt-C(12)-C(13)	74.7 (6)	71.9 (5)
Pt-C(12)-C(15)	124.5 (8)	127.1 (9)
C(11)-C(12)-C(13)	108 (1)	106 (1)
C(11)-C(12)-C(15)	126 (1)	128 (1)
C(13)-C(12)-C(15)	126 (1)	125 (2)
Pt-C(13)-C(12)	70.0 (7)	72.4 (5)
Pt-C(13)-C(14)	126.9 (8)	125.4 (7)
C(12)-C(13)-C(14)	128 (1)	129 (1)
C(12)-C(13)-C(13)'	108 (1)	109 (1)
C(13)-C(13)-C(14)	124 (1)	122 (1)

^aSee footnote at Table III.

Reaction of 4 with Br₂. As with the analogous reaction for 1, a 5-mm NMR tube was loaded with 0.035 g of Tp*PtMe₃, and 3 equiv or more of Br₂ was injected. The ¹H NMR spectrum showed only changes consistent with bromination of the 4-H position of the three pyrazolyl rings.

¹H NMR (CDCl₃), δ: 2.61 (9 H, s), 2.41 (9 H, s), 1.50 (9 H, m), ²J_{Pt-H} = 86 Hz). IR: ν_{B-H} = 2528 cm⁻¹.

Collection and Reduction of X-ray Data. Crystals of 2, dimensions 0.4 × 0.3 × 0.1 mm, and 3, dimensions 0.3 × 0.3 × 0.1 mm, from the preparations above were selected and mounted on glass fibers. Data were collected at ambient temperatures on an Enraf-Nonius CAD4 computer controlled diffractometer with graphite-monochromatized Mo Kα radiation. Cell constants were determined by a least-squares fit to the centered angular coordinates of 24 intense reflections with 2θ values between 16 and 37°. An empirical absorption correction based on six ψ scans was applied. The intensities of three standard reflections remeasured every 120 min showed no decay. Crystallographic data for 2 and 3 are summarized in Table SI (supplementary material) and Table I.

Structure Solution and Refinement. The structures of 2 and 3 were solved by a combination of Patterson and direct methods.²⁸ For both structures, systematic absences indicated the space group P2₁ or P2₁/m. For 2, refinement in the centrosymmetric setting was straightforward. Attempts to refine 3 in the noncentrosymmetric space group P2₁ indicated a disorder of the Me and Br positions with large correlations between the positions related by the mirror in the centric space group (the occupancy of Br(2) in both positions refined to ~0.5). The centric space group P2₁/m was therefore also chosen for 3 with a disorder of the Me and one Br across the mirror plane.

(28) SHELX-86: Sheldrick, G. M. In *Crystallographic Computing 3*; Sheldrick, G. M., Kruger, C., Goddard, R., Eds.; Oxford University Press: Oxford, U.K., 1985.

In the case of 2, hydrogen atoms were included at their calculated positions (C–H = 0.95 Å) and were not refined. Hydrogen atoms were not included for 3. The final difference Fourier map for 3 showed no peaks greater than 0.5 e/Å³ except for several peaks between 0.5 and 1.9 e/Å³ within 1 Å of the platinum. The final difference Fourier map for 2 showed several noise peaks as high as 5 e/Å³ within 1 Å of the platinum. This may be due to a stacking disorder as observed in the wide mosaic for 2. Several crystals were examined, and all showed high mosaic spread along *b*. Two complete data sets on two crystals were collected. The results for one were marginally better, and this is the set reported. Final positional parameters and bond distances and angles are listed in Tables II–V. Anisotropic thermal parameters for non-hydrogen atoms of 2 and 3 are given in Tables SII and SIII, positional and thermal parameters for the hydrogen atoms of 2 are listed in Table SIV, and observed and calculated structure factors are listed in Tables SVI and SVII (all supplementary material).

Acknowledgment. The support of this work by the Division of Chemical Sciences, Office of Basic Energy Sciences, Office of Energy Research, U.S. Department of Energy (Contract DE-FG02-88ER13880), and ARCO Chemical Co. is gratefully acknowledged. We thank Dr. Charles L. Barnes for assistance with the crystal structure determinations.

Supplementary Material Available: Crystal data collection and reduction parameters for 2 and 3 (Table SI), anisotropic thermal parameters for non-hydrogen atoms of 2 and 3 (Tables SII and SIII), positional and thermal parameters for the hydrogen atoms of 2 (Table SIV), and least-squares planes for the C₅ ring of 2 (Table SV) (5 pages); observed and calculated structure factors for 2 and 3 (Tables SVI and SVII) (10 pages). Ordering information is given on any current masthead page.

Contribution from the Department of Chemistry,
The University of Alberta, Edmonton, Alberta, Canada T6G 2G2

Dithiophosphate-Bridged Ruthenium(I) and Ruthenium(II) Complexes. Structure of [Ru₂(CO)₄(μ-S₂PMe₂)₂(PPh₃)₂]^{1/2}·CH₂Cl₂

Robert W. Hilt and Martin Cowie*

Received February 9, 1990

Replacement of the bridging acetate groups in [Ru₂(CO)₄(μ-O₂CMe)₂(PR'₂R'')₂] (R', R'' = Ph, Me) by the dithiophosphate anions R₂PS₂⁻ (R = Me, Ph) yields a new class of dithiophosphate-bridged Ru(I) complexes, [Ru₂(CO)₄(μ-S₂PR₂)(PR'₂R'')₂]. Although the Ru–Ru bond in these species can be reversibly protonated, it does not react with [Au(PPh₃)]⁺[BF₄]⁻, diazomethane, or dimethyl acetylenedicarboxylate. Reaction of the related acetate-bridged species [Ru₂(CO)₄(μ-O₂CMe)₂(NCMe)₂] with NaS₂PMe₂ does not yield the expected dithiophosphate-bridged product but instead gives the mononuclear species [Ru(CO)₂(η²-S₂PMe₂)₂] along with Na₂S, NaO₂CMe, MeCN, and Me₂P(S)P(S)Me₂. An X-ray structure determination of [Ru₂(CO)₄(μ-S₂PMe₂)₂(PPh₃)₂]^{1/2}·CH₂Cl₂ confirms the dithiophosphate-bridged formulation and shows a long Ru–Ru separation of 2.9000 (6) Å and a twisting about the metal–metal axis by ca. 39°. This compound crystallizes in the monoclinic space group P2₁/c with cell parameters *a* = 15.182 (3) Å, *b* = 18.230 (4) Å, *c* = 18.082 (4) Å, β = 94.23 (2)°, and *Z* = 4. Refinement has converged at *R* = 0.054 and *R*_w = 0.082 on the basis of 5928 unique reflections and 365 parameters varied.

Introduction

Dialkyl- and diaryldithiophosphate anions, R₂PS₂⁻, have proven to be versatile ligands that can bind in either a unidentate,^{1–10} chelating,^{1–22} or bridging^{23–25} fashion to a wide range of

transition metals. Of these binding modes, the chelating one is the most common, while complexes containing bridging R₂PS₂⁻

- (1) Cole-Hamilton, D. J.; Stephenson, T. A. *J. Chem. Soc., Dalton Trans.* **1974**, 739.
- (2) Robertson, D. R.; Stephenson, T. A. *J. Organomet. Chem.* **1976**, 107, C46.
- (3) Faraone, F.; Marsala, V. *Inorg. Chim. Acta* **1976**, 17, 217.
- (4) Cole-Hamilton, D. J.; Stephenson, T. A. *J. Chem. Soc., Dalton Trans.* **1976**, 2396.
- (5) Alison, J. M. C.; Gould, R. O.; Stephenson, T. A. *J. Chem. Soc. A* **1971**, 3690.
- (6) Faithful, B. L.; Stephenson, T. A. *J. Chem. Soc. A* **1970**, 1504.
- (7) Alison, J. M. C.; Fackler, J. P., Jr.; Fraser, A. J. F.; Gould, R. O.; Lin, I. J. B.; Stephenson, T. A.; Thompson, L. D. *Inorg. Chem.* **1982**, 21, 2397.
- (8) Colton, R.; Stephenson, T. A. *Polyhedron* **1984**, 3, 231.
- (9) Cornock, M. C.; Stephenson, T. A. *J. Chem. Soc., Dalton Trans.* **1977**, 501.

- (10) Faraone, F.; Piraino, P. *Inorg. Chim. Acta* **1976**, 16, 89.
- (11) Cole-Hamilton, D. J.; Owen, J. D. *J. Chem. Soc., Dalton Trans.* **1974**, 1867.
- (12) Appel, D. M.; Boyd, A. S. F.; Robertson, I. W.; Roundhill, D. M.; Stephenson, T. A. *Inorg. Chem.* **1982**, 21, 449.
- (13) Gogoi, P. K.; Mukherjee, R. N.; Shankar, S. *Polyhedron* **1985**, 4, 1717.
- (14) Cole-Hamilton, D. J.; Robertson, D. R.; Stephenson, T. A. *J. Chem. Soc., Dalton Trans.* **1975**, 1260.
- (15) Sime, W. J.; Stephenson, T. A. *J. Chem. Soc., Dalton Trans.* **1978**, 1647.
- (16) Byers, W.; Cavell, R. G.; Day, E. D. *Inorg. Chem.* **1971**, 10, 2710.
- (17) Byers, W.; Cavell, R. G.; Day, E. D.; Watkins, P. M. *Inorg. Chem.* **1971**, 10, 2716.
- (18) Kuchen, W.; Judat, A. *Chem. Ber.* **1967**, 100, 991.
- (19) Cole-Hamilton, D. J.; Stephenson, T. A. *J. Chem. Soc., Dalton Trans.* **1974**, 1818.
- (20) Cornock, M. C.; Gould, R. O.; Jones, C. L.; Stephenson, T. A. *J. Chem. Soc., Dalton Trans.* **1977**, 1307.
- (21) Lindner, E.; Matejcek, K.-M. *J. Organomet. Chem.* **1972**, 34, 195.